GREEN SYNTHESIS OF nZVI/GNP NANOCOMPOSITE AS AN OXIDATION CATALYST FOR RHODAMINE B DEGRADATION IN AQUEOUS MEDIUM

TỔNG HỢP XANH VẬT LIỆU NANOCOMPOSITE nZVI/GNP XÚC TÁC OXY HÓA PHÂN HỦY RHODAMINE B TRONG MÔI TRƯỜNG NƯỚC

Nguyen Manh Ha[1], Nguyen Duc Kien[1], Le Hai Yen[1], Nguyen Thu Trang[1], Vu Minh Chau[2], Nguyen Thi Hoai Phuong[2,*]

DOI: http://doi.org/10.57001/huih5804.2025.145

ABSTRACT

The advancement of sustainable nanomaterials for wastewater remediation has garnered considerable interest in recent years. This study successfully produced a nano zero-valent iron/graphene nanoplatelet (nZVI/GNP) nanocomposite using a green synthesis approach and assessed its efficacy as an oxidation catalyst for the degradation of Rhodamine B (RhB) in an aqueous environment. The synthesized nZVI/GNP shown exceptional catalytic performance, attaining over 90% elimination of RhB after 120 minutes, owing to improved electron transport and reactive oxygen species (ROS) production resulting from the synergistic interactions between nZVI and GNP. Kinetic analysis revealed that RhB degradation adhered to a pseudo-second-order kinetic model ($R^2 = 0.97863$), signifying chemisorption as the prevailing process. The second-order rate constant $k_2 = 0.00119$L/g·min was markedly greater than the first-order rate constant $k_1 = 0.04944$min^{-1}, hence affirming the enhanced catalytic efficacy of nZVI/GNP. The green synthesis method not only mitigates environmental effect but also improves the stability and reactivity of nZVI, rendering it a viable option for sustainable water treatment applications. This research underscores the efficacy of nZVI/GNP as a powerful oxidation catalyst for the elimination of organic pollutants. Future study should concentrate on enhancing the synthesis method, expanding its applicability, and evaluating the long-term stability and recyclability of the nanocomposite for effective wastewater treatment.

Keywords: *nZVI/GNP nanocomposite, Rhodamine B, Fenton-like oxidation, wastewater treatment, advanced oxidation process (AOP).*

TÓM TẮT

Sự tiến bộ của vật liệu nano bền vững để phục hồi nước thải đã thu hút được sự quan tâm đáng kể trong những năm gần đây. Nghiên cứu này đã sản xuất thành công nanocomposite sắt/graphene hóa trị không (nZVI/GNP) bằng cách sử dụng phương pháp tổng hợp xanh và đánh giá hiệu quả của nó như một chất xúc tác oxy hóa để phân hủy Rhodamine B (RhB) trong môi trường nước. nZVI/GNP tổng hợp cho thấy hiệu suất xúc tác đặc biệt, đạt được hơn 90% loại bỏ RhB sau 120 phút, nhờ cải thiện vận chuyển điện tử và sản xuất các loài oxy phản ứng (ROS) do tương tác hiệp đồng giữa nZVI và GNP. Phân tích động học cho thấy sự phân hủy RhB tuân thủ theo mô hình động học bậc hai giả ($R^2 = 0,97863$), biểu thị sự hấp phụ hóa học là quá trình chủ đạo. Hằng số tốc độ bậc hai $k_2 = 0,00119$L/g·min lớn hơn đáng kể so với hằng số tốc độ bậc nhất $k_1 = 0,04944$min^{-1}, do đó khẳng định hiệu quả xúc tác được tăng cường của nZVI/GNP. Phương pháp tổng hợp xanh không chỉ làm giảm tác động đến môi trường mà còn cải thiện độ ổn định và khả năng phản ứng của nZVI, biến nó thành một lựa chọn khả thi cho các ứng dụng xử lý nước bền vững. Nghiên cứu này nhấn mạnh hiệu quả của nZVI/GNP như một chất xúc tác oxy hóa mạnh mẽ để loại bỏ các chất ô nhiễm hữu cơ. Các nghiên cứu trong tương lai nên tập trung vào việc tăng cường phương pháp tổng hợp, mở rộng khả năng ứng dụng của nó và đánh giá độ ổn định và khả năng tái chế lâu dài của nanocomposite để xử lý nước thải hiệu quả.

Từ khóa: *Nanocomposite nZVI/GNP, Rhodamine B, oxy hóa giống Fenton, xử lý nước thải, quy trình oxy hóa tiên tiến.*

[1]Faculty of Chemical Technology, Hanoi University of Industry, Vietnam
[2]Joint Vietnam - Russia Tropical Science and Technology Research Center, Vietnam
[*]Email: hoaiphuong1978@gmail.com
Received: 25/2/2025
Revised: 18/5/2025
Accepted: 28/5/2025

1. INTRODUCTION

Because of their long-lasting nature and the possibility of being poisonous, synthetic dyes are a major source of water pollution, a serious environmental concern. Rhodamine B (RhB), a widely utilized xanthene dye, is present in a wide variety of applications, including biological staining, cosmetics, and textiles. However, due to its resistance to traditional wastewater treatment techniques, RhB poses environmental and human health concerns. As a result, the development of technologies that are both effective and sustainable for the degradation of RhB is essential. Various degradation technologies have been explored to remove RhB from aqueous solutions, including physical, chemical, and biological approaches. In Nidheesh et. al.'s study, RhB removal using a graphite-graphite electro-Fenton system was optimized at 8V and 4 - 5cm electrode spacing, achieving 99.2% removal in 180 min, with efficiency influenced by electrode area, immersion depth, and dye concentration [1]. In Muhammad et al.'s research, the discharge of RhB from wastewater by employing NaOH-treated rice husk reached 83%, with the adsorption capacity being 1.66mg/g [2]. Krzysztof et al. compared four minerals (zeolite, halloysite, chalcedonite, and Devonian sand) for RhB adsorption with zeolite showing the highest capacity (6.964mg/g) [3]. Maedeh et al. used palm shell-derived activated carbon (476.8m^2/g BET) for RhB removal, achieving 95% efficiency under optimal conditions (62.6µmol/L, pH 3, 50°C) [4]. Seyyed et al. used stalk corn-based activated carbon (SCBAC) for RhB removal, achieving a maximum adsorption capacity of 5.6mg/g at optimal conditions (pH 3, 2.5g/L dosage) [5].

The capacity of nanoscale zero-valent iron (nZVI) to degrade organic pollutants through redox reactions and catalytic oxidation has garnered a significant amount of attention in recent years. nZVI possesses the capability to decompose various chlorinated chemicals and is extensively employed for the treatment of contaminated water [6-8]. However, the particles of nZVI have a tendency to agglomerate, which decreases their reactivity and stability. Nanocomposites that incorporate carbon-based materials, such as biochar activated carbon, carbon nanotubes, and graphene, have been investigated as a means of improving dispersion and catalytic performance in order to circumvent this constraint [9-12]. Graphene nanoplatelets (GNPs) are a class of carbon-based nanomaterials composed of multiple layers of graphene with lateral dimensions in the micrometer range and thicknesses in the nanometer scale. They exhibit exceptional electrical, thermal, and mechanical properties, making them valuable in various applications, including catalysis, energy storage, and environmental remediation [13-15]. As a result of its high surface area, superior conductivity, and robust interaction with iron nanoparticles, graphene nanoplatelet (GNP) improve electron transport and overall degrading performance for the nZVI composite.

In this study, we synthesized an nZVI/GNP nanocomposite and investigated its catalytic activity for RhB degradation in an aqueous medium. The synergistic effect between nZVI and GNP was evaluated in terms of degradation efficiency, reaction kinetics, and potential mechanisms. This work contributes to the development of advanced nanocomposite catalysts for wastewater treatment, offering a promising approach for the removal of persistent organic pollutants.

2. MATERIALS AND METHODS

2.1. Preparation of *Terminalia catappa* leaf extract

Terminalia catappa leaves that were fresh were gathered from the city of Ha Noi in the country of Vietnam. The *Terminalia catappa* leaves were cleaned by washing them with deionized (DI) water, and then they were dried and milled into a powder. After that, five grams of the dried leaves were dispersed in 100mL of ethanol (C_2H_5OH, more than 99.7%, China) by means of ultrasonication for 60 minutes. A vacuum filtering system was used to collect the extract after the reducing agent was extracted at a temperature of 60°C for two hours. The *Terminalia catappa* leaf extract that was obtained was diluted with DI water at a ratio of 1:20, and the solution that was obtained was utilized as a reducing agent for the reduction of Fe ions.

2.2. Preparation of nZVI/GNP composite

Weigh 6.75g of $FeCl_3{\cdot}6H_2O$ and transfer it to a flask. Add 25mL of distilled water to the flask and stir to ensure complete mixing. Utilize ultrasonography to verify full disintegration. Introduce 0.2g of GNP into 50mL of $FeCl_3$ solution and sonicate for 30 minutes. The gradual addition of 50mL of *Terminalia catappa* leaf extract while stirring for 2 hours. Permit the mixture to repose overnight. Following the overnight period, filter the mixture and purify the resultant substance with an ethanol/water solution; then, centrifuge at 8000rpm for 15 minutes to produce the precipitate.

2.3. Characterization of nZVI/GNP composite

The infrared (IR) spectra of the substance were acquired using an FT-IR spectrometer in the range of 400

- 4000cm^{-1}. Scanning electron microscopy (SEM) was employed to visualize the surface and morphologies of the nZVI/GNP composite. X-ray diffraction (XRD) patterns of the powder were obtained using a diffractometer employing CuKα radiation at 15mA and 40kV.

2.4. Rhodamine B removal

The degradation of Rhodamine B (RhB) using nZVI/GNP was conducted under controlled laboratory conditions to evaluate the catalytic efficiency of the material. In a typical experiment, a known concentration of RhB solution (typically ranging from 2.5 to 15mg/L) was prepared in a fixed volume, commonly 100mL. A specific amount of nZVI/GNP catalyst (from 0.05 to 0.30g/L) was then added to the solution, and the mixture was stirred at a constant speed (typically 150 - 200rpm) at room temperature. At predetermined time intervals (0, 10, 20, 30,..., 120 minutes), samples were withdrawn and immediately filtered or centrifuged to remove the solid catalyst. The remaining concentration of RhB in the solution was measured using a UV-Vis spectrophotometer at the maximum absorbance wavelength of 553nm.

The efficiency of RhB removal on nZVI/GNP was calculated by the following equation:

$$H\,\% = \frac{(C_0 - C_t)}{C_0} \times 100\% \quad (1)$$

where C_0 and C_t (mg/L) are the initial and residual RhB concentrations, respectively.

The first-order kinetic model was employed to simulate experimental data to ascertain the surface photodegradation rate constant:

$$\frac{C_t}{C_0} = e^{-k_1 t} \quad (2)$$

The second-order kinetic model was utilized to simulate the elimination kinetics of RhB by nZVI/GNP in solution:

$$\frac{C_t}{C_0} = \frac{1}{1 + k_2 . C_0 . t} \quad (3)$$

where C_0, C_t (ppm) are concentration of RhB at intial and t moment, respectively; k_1 (min^{-1}) is the pseudo-first-order rate constant; k_2 (L.(mg.min)$^{-1}$) is the pseudo-second-order rate constant.

3. RESULTS AND DISCUSSION

3.1. Characterization of nZVI/GNP composite

Figure 1 presents SEM images depicting the morphology of a nZVI/GNP (nanoscale zero-valent iron/graphene nanoplatelet) composite at various magnifications. At a magnification of 10,000x, the graphene nanoplatelets (GNP) manifest as slender, stratified, and crumpled sheet-like formations. The nZVI particles are dispersed over the GNP surface, creating agglomerates in certain regions. The sheet-like structure of GNP offers a substantial surface area, advantageous for stabilizing nZVI particles and mitigating excessive aggregation. At a magnification of 50,000x, a detailed examination uncovers spherical nZVI nanoparticles, which manifest as clusters or chains, likely attributable to magnetic interactions. The significant dispersion of nZVI on the GNP surface indicates a robust interaction, perhaps augmenting reactivity and stability. The diminutive particle size of nZVI enhances its surface reactivity, rendering it beneficial for environmental applications, including pollutant removal. The composite structure indicates that GNP functions as a support matrix, diminishing nZVI aggregation and enhancing its dispersibility. The observed morphology validates the effective synthesis of the nZVI/GNP composite, indicating possible applications in water treatment, dye removal, or environmental remediation.

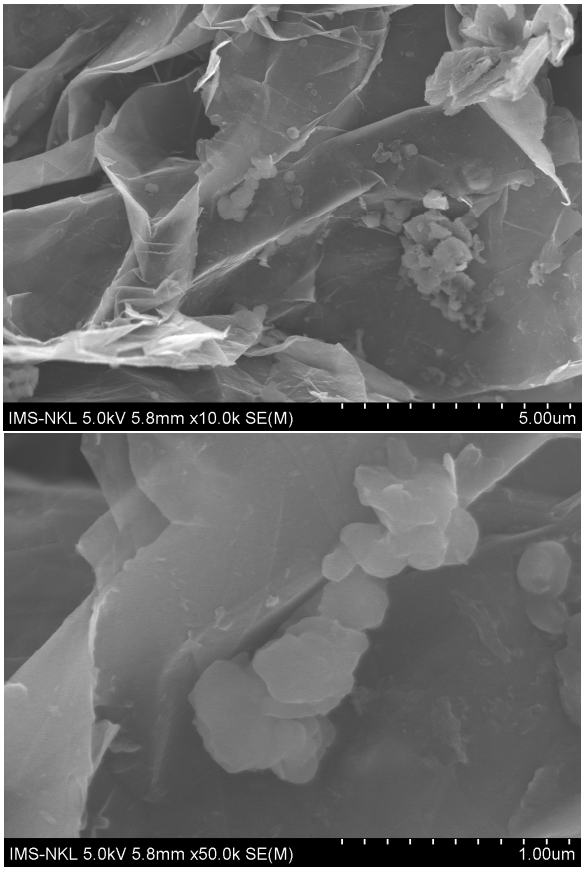

Figure 1. SEM images of nZVI/GNP composite

The graphene nanoplatelets (GNP, blue) and a composite of nanoscale zero-valent iron on graphene nanoplatelets (nZVI/GNP, yellow) are compared in the X-ray diffraction (XRD) patterns that are displayed in Figure

2. Graphitic nanoparticles (GNP) exhibit a prominent peak at around 26.6^0 (2θ), which corresponds to the (002) diffraction plane of graphitic carbon. The presence of this peak is indicative of the distinctive structure of graphene nanoplatelets. Some structural disorder or probable contaminants may be present, as indicated by the presence of additional small peaks in the lower 2θ range. While the peak at approximately 26.6^0 is still evident with the nZVI/GNP composite, it has been significantly decreased. This suggests that the graphene structure is still present, but it may be altered as a result of the nZVI deposition which has been applied. The presence of zero-valent iron (Fe^0) is confirmed by the appearance of a conspicuous peak at approximately 44.71^0, which corresponds to the (110) plane of body-centered cubic (BCC) iron [16]. The creation of the nZVI phase on the graphene surface is suggested by the fact that the total intensity of peaks is higher than that of pure graphene nanoparticles (GNP). Additionally, distinct peaks at 2θ ≈ 35.2°, 39.8°, and 53.1° correspond to the characteristic reflections of β-FeOOH (akaganeite), with the most intense peak at 35.2°, attributed to the (310) plane. This phase coexists with Fe^0 nanoparticles when synthesized using iron chloride salt, as chloride ions facilitate its tunnel-like structure formation. As a result of the existence of Fe^0 peaks, the XRD results provide proof that the synthesis of the nZVI/GNP composite was successful. The decrease in strength of the GNP peak at approximately 26.6^0 implies interactions between nZVI and graphene, which may have an effect on stacking or dispersion. The absence of significant iron oxide peaks is indicative of the fact that the material is primarily composed of Fe^0 rather than oxidized forms; yet, it is possible that some amorphous oxide layers are still present.

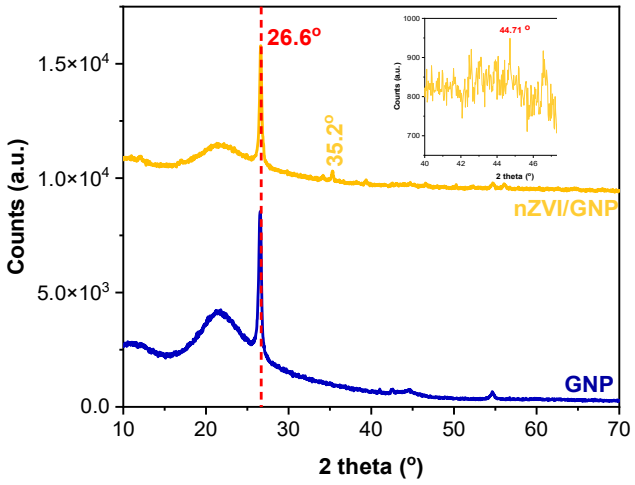

Figure 2. The XRD patterns of GNP (blue) and nZVI/GNP composite (yellow)

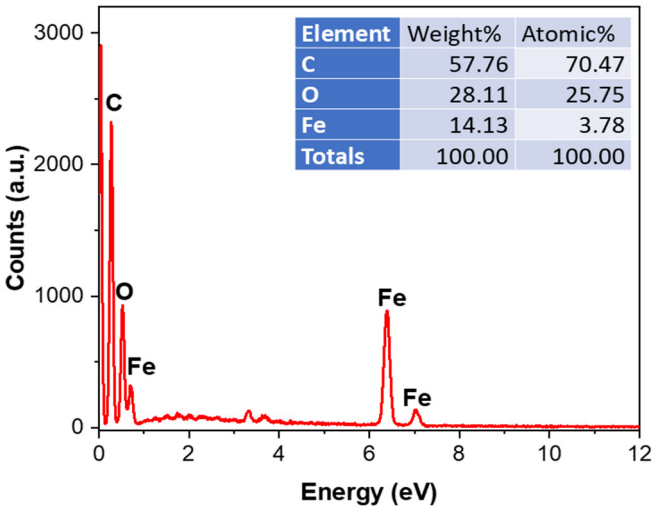

Figure 3. The EDX patterns of nZVI/GNP composite

Figure 3 presents the EDX spectrum, which offers an elemental analysis of the nZVI/GNP composite. The elemental composition indicates that carbon constitutes 57.76%, so affirming that the elevated carbon content corroborates the presence of graphene nanoplatelets (GNP) as the principal structural element of the composite. The oxygen level is 28.11%, indicating the presence of oxygen and suggesting the partial oxidation of nZVI, possibly resulting in the formation of FeOOH species. Oxygen may also originate from functional groups on GNP, including hydroxyl (-OH) and carboxyl (-COOH) groups. The presence of 14.13% weight iron and the Fe peaks validate the integration of nanoscale zero-valent iron (nZVI) within the composite. The reduced atomic percentage of Fe indicates that nZVI is uniformly distributed within the GNP matrix, rather than aggregating into huge clusters. The spectrum has distinct Fe peaks at around 0.7 eV, 6.4 eV, and 7.1 eV, indicative of iron. The pronounced C peak (~0.3 eV) is associated with the GNP structure. The O peak (~0.5 eV) further corroborates the existence of iron oxides or oxygen-containing moieties. The elevated carbon content verifies that GNP is the predominant phase in the composite. The presence of oxygen indicates partial oxidation of Fe^0, potentially influencing the material's reactivity and stability. The modest iron level (14.13 wt%) signifies that nZVI particles are effectively incorporated into the GNP matrix. The composite structure indicates that GNP serves as a support, facilitating the dispersion of Fe nanoparticles and possibly augmenting their efficacy in environmental or catalytic applications.

Figure 4 displays FTIR spectra that elucidate the functional groups in GNP and nZVI/GNP composites. At

GNP Spectrum, 2988cm^{-1}, a faint peak corresponds to C-H stretching vibrations, perhaps originating from residual organic impurities or functional groups on the GNP surface. 1066cm^{-1} signifies C–O stretching, denoting the existence of oxygen-containing functional groups (e.g., epoxy, hydroxyl, or carboxyl groups). The extensive absorption in the 1000 - 1500cm^{-1} region indicates C=C vibrations, typical of graphitic materials. In the nZVI/GNP Spectrum, a novel peak at 485cm^{-1} is observed exclusively in the nZVI/GNP composite, which can be ascribed to the Fe-O stretching vibration, signifying the partial oxidation of Fe(0) to FeOOH. The 1066cm^{-1} (C-O stretching) peak in GNP exhibits diminished intensity, indicating that the interaction of nZVI with GNP may have altered the surface oxygen-containing groups. The GNP spectrum verifies the existence of oxygen-functionalized graphene structures. The Fe-O peak at 485cm^{-1} in the nZVI/GNP composite indicates the partial oxidation of Fe^0 resulting from exposure to air or water. The reduction in C-O peak intensity in the composite suggests that nZVI particles may have engaged with oxygen-containing groups on GNP, perhaps promoting chemical bonding or charge transfer interactions. The data validate the successful integration of nZVI onto GNP, while also suggesting a certain extent of Fe oxidation, which may affect reactivity in applications like environmental remediation or catalysis.

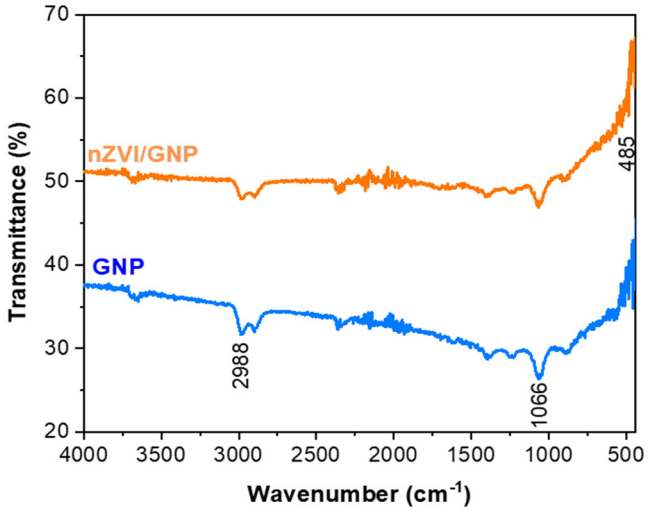

Figure 4. The FTIR spectroscopy of GNP (blue) and nZVI/GNP composite (yellow)

3.2. Rhodamine B removal

The effect of initial RhB concentration on its degradation by nZVI/GNP was investigated, as shown in Figure 5. At lower concentrations (2.5 - 7.5mg/L), the degradation efficiency (H%) increased rapidly, reaching over 90% within 120 minutes, indicating that sufficient active sites were available on the nZVI/GNP surface to effectively interact with dye molecules. The degradation rate was notably high in the initial 30 minutes, suggesting fast adsorption and reduction reactions under low pollutant loading. However, as the initial concentration increased to 10.0 - 15.0mg/L, the removal efficiency decreased significantly. At 15.0mg/L, only about 70% degradation was achieved after 120 minutes. This decline is attributed to the saturation of reactive sites and increased competition among dye molecules for adsorption, which slows down the overall reaction rate. Moreover, higher dye concentrations may result in the accumulation of intermediate products that interfere with the degradation process or hinder the diffusion of reactive species, such as Fe^{2+} ions and hydroxyl radicals, into the bulk solution. At high concentrations, the increased density of RhB molecules may enhance the chances of molecular interactions. However, this can lead to diffusion limitations and uneven distribution, which ultimately reduces the effective interaction between RhB molecules and the reactive sites on nZVI/GNP. These findings suggest that the degradation efficiency of RhB by nZVI/GNP is inversely related to its initial concentration, emphasizing the importance of optimizing dye loading in real wastewater applications to achieve maximum treatment performance.

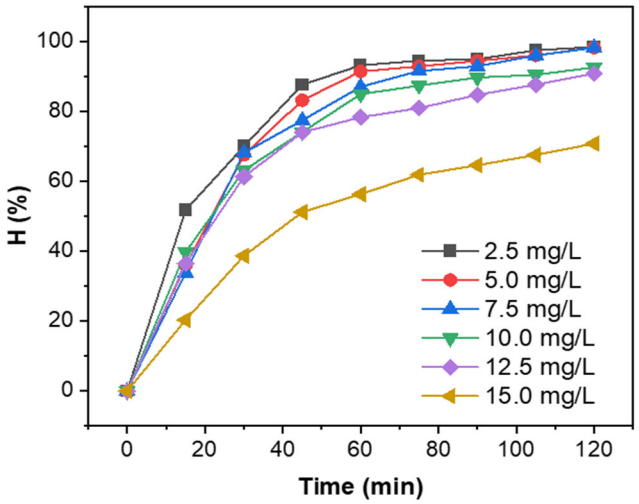

Figure 5. Effect of initial concentration on degradation rate of RhB with nZVI/GNP

Figure 6 presents the effect of nZVI/GNP dosage on the degradation efficiency (H%) of RhB over time. As the dosage increases from 0.05 to 0.30g/L, a significant enhancement in degradation efficiency is observed. At the lowest dosage (0.05g/L), the removal efficiency

reaches only about 70% after 120 minutes, indicating limited availability of active sites for RhB interaction. With increasing dosage, especially from 0.10 to 0.25g/L, the degradation rate improves markedly due to the increased surface area and availability of reactive sites, which promote more effective adsorption and redox reactions with RhB molecules. The fastest degradation occurs within the first 20 - 40 minutes, particularly at higher dosages. However, beyond 0.25g/L, the improvement in degradation efficiency becomes less pronounced, as seen in the curves for 0.25 and 0.30g/L which nearly overlap. This plateau effect suggests that excessive nZVI/GNP may lead to particle aggregation, reducing the effective surface area and possibly scavenging reactive species. Overall, the results indicate that increasing the nZVI/GNP dosage enhances RhB removal efficiency up to an optimal point, beyond which further addition provides minimal benefit. This highlights the importance of optimizing material dosage for cost-effective and efficient wastewater treatment using nanomaterials.

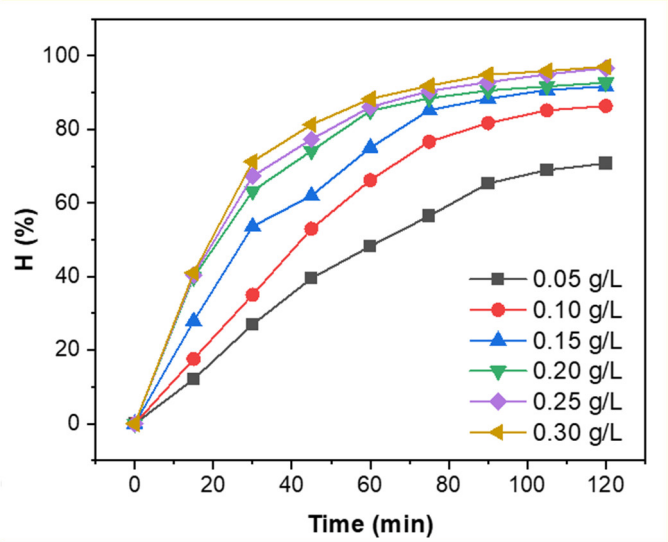

Figure 6. Effect of dosage on degradation rate of RhB with nZVI/GNP

Figure 7 depicts the temporal degradation of Rhodamine B (RhB) under irradiation with nZVI/GNP. The initial RhB concentration is 10.1259mg/L, and within the first 30 minutes, the C_t exhibits a significant decline, signifying a swift early degradation phase. After 120 minutes, C_t attains around 0.7388mg/L, indicating significant RhB elimination. The degrading efficiency (H) exhibits an upward trend, surpassing 92% after 120 minutes. The majority of degradation transpires within the initial 60 minutes, after which the rate of efficiency enhancement diminishes, likely due to a reduced number of remaining RhB molecules and the saturation of active sites. The abrupt initial decline in RhB concentration indicates a pseudo-first-order response, wherein the degradation rate correlates with the residual RhB concentration. The deterioration curve stabilizes after 90 minutes, suggesting the potential establishment of reaction equilibrium or catalyst deactivation. The nZVI/GNP system demonstrates exceptional efficacy in degrading RhB, with over 90% elimination within 120 minutes. The reaction occurs most rapidly within the initial 30 - 60 minutes and then decelerates, indicating an ideal duration for effective treatment. Additional optimization may concentrate on enhancing reaction efficiency beyond 60 minutes or augmenting catalyst stability.

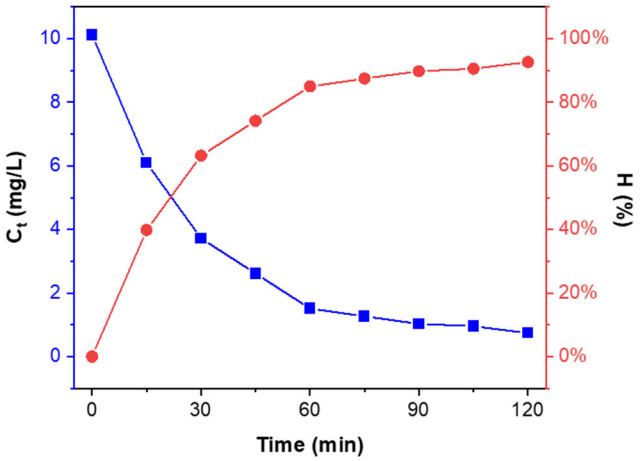

Figure 7. The degradation efficiency of RhB vs irradiation time with nZVI/GNP

Figure 8 illustrates two kinetic models, pseudo-first-order and pseudo-second-order, for the degradation of RhB utilizing nZVI/GNP. The slope of the fitted line in pseudo-first-order kinetics yields $k_1 = 0.04944\ min^{-1}$. The coefficient of determination R^2 is 0.94793, signifying a strong fit, albeit not flawless. In the context of pseudo-second-order kinetics, the slope of the fitted line yields $k_2 = 0.00119 L/g{\cdot}min$. The R^2 value is 0.97863, surpassing that of the first-order model, signifying a superior fit. The pseudo-second-order model demonstrates a superior R^2 value (0.97863 compared to 0.94793), indicating that RhB degradation by nZVI/GNP adheres more closely to second-order dynamics. The elevated correlation in the pseudo-second-order model suggests that the degradation process may be governed by chemisorption instead of merely mass transfer or diffusion mechanisms. The pseudo-first-order model remains a satisfactory fit, suggesting that certain elements of the process may be governed by a diffusion-limited step. The degradation of

RhB by nZVI/GNP seems to adhere more closely to a pseudo-second-order kinetic mechanism, indicating a more robust connection between RhB molecules and the active adsorption sites on the material.

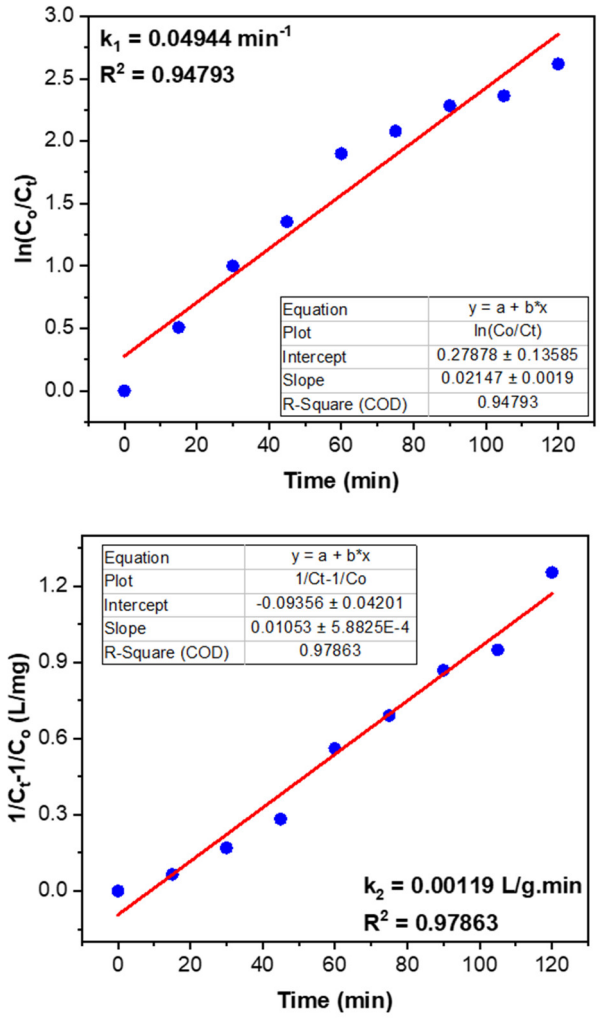

Figure 8. The first-pseudo order (left) and second-pseudo order (right) models of RhB degradation on nZVI/GNP

4. CONCLUSION

This study successfully produced a nano zero-valent iron/graphene nanoplatelet (nZVI/GNP) nanocomposite via a green synthesis method and assessed its catalytic efficacy for the degradation of Rhodamine B (RhB) in an aqueous environment. The synthesized nanocomposite demonstrated significant catalytic efficiency, owing to the synergistic interactions between nZVI and GNP, which improved electron transport and the formation of reactive oxygen species (ROS). The nZVI/GNP system exhibits remarkable effectiveness in degrading RhB, achieving over 90% removal after 120 minutes. Kinetic study demonstrated that RhB degradation adhered to a pseudo-second-order kinetic model (R^2 = 0.97863), suggesting that chemisorption was the predominant mechanism in the degradation process. The reaction rate constants further validated the catalyst's efficacy, with the second-order rate constant k_2 = 0.00119L/g·min markedly exceeding the first-order model's k_1 = 0.04944 min^{-1}. The data indicate that nZVI/GNP functions as an efficient oxidation catalyst, promoting the degradation of RhB in aqueous environments. This study's green synthesis method diminishes environmental effect while improving the stability and reactivity of nZVI. This method is consistent with sustainable water treatment methods and presents a viable solution for eliminating organic contaminants from contaminated water sources. Future investigations should concentrate on refining the synthesis method, enhancing the application scale, and evaluating the long-term stability and recyclability of the nanocomposite for effective wastewater treatment.

REFERENCES

[1]. Nidheesh P., Gandhimathi R. J. D.,Treatment W., "Removal of Rhodamine B from aqueous solution using graphite–graphite electro-Fenton system," *Desalination and Water Treatment,* 52, 1872-1877, 2014.

[2]. Khan M. I., Shanableh A. J. D., Treatment W., "Adsorption of Rhodamine B from an aqueous solution onto NaOH-treated rice husk," *Desalination and Water Treatment,* 254, 104-115, 2022.

[3]. Kuśmierek K., Fronczyk J., Świątkowski A. J. W., "Adsorptive removal of rhodamine B dye from aqueous solutions using mineral materials as low-cost adsorbents," *Water Air Soil Pollut,* 234, 531, 2023.

[4]. Mohammadi M., Hassani A. J., Mohamed A. R., Najafpour G. D., "Removal of rhodamine B from aqueous solution using palm shell-based activated carbon: adsorption and kinetic studies," *Journal of Chemical & Engineering Data*, 55, 5777-5785, 2010.

[5]. Mousavi S. A., Kamarehie B., Almasi A., Darvishmotevalli M., Salari M., Moradnia M., Azimi F., Ghaderpoori M., Neyazi Z., Karami M., "Removal of Rhodamine B from aqueous solution by stalk corn activated carbon: Adsorption and kinetic study," *Biomass Conv. Bioref.*, 13, 7927-7936, 2023.

[6]. Salom D., Fernández-Verdejo D., Moral-Vico J., Font X., Marco-Urrea E., "Combining nanoscale zero-valent iron and anaerobic dechlorinating bacteria to degrade chlorinated methanes and 1, 2-dichloroethane," *Environ Sci Pollut Res,* 30, 45231-45243, 2023.

[7]. Bae S., Lee W., "Influence of riboflavin on nanoscale zero-valent iron reactivity during the degradation of carbon tetrachloride," *Environmental Science & Technology*, 48, 2368-2376, 2014.

[8]. Ferrari G. A., de Oliveira Cruz F. S., Moreira R. P. L., Puiatti G. A., de Miranda Moraes L. D., Oliveira A. F., "Development of a method to evaluate

the efficiency of nanoscale zero-valent iron (nZVI) to degrade pollutants," *The Journal of Engineering and Exact Sciences*, 5, 0299-0307f, 2019.

[9]. Quan G., Sun W., Yan J., Lan Y., "Nanoscale zero-valent iron supported on biochar: characterization and reactivity for degradation of acid orange 7 from aqueous solution," *Water Air Soil Pollut,* 225, 1-10, 2014,

[10]. Iran Manesh M., Sohrabi M. R., Mortazavi Nik S., "Nanoscale zero-valent iron supported on graphene novel adsorbent for the removal of diazo direct red 81 from aqueous solution: isotherm, kinetics, and thermodynamic studies," *Iranian Journal of Chemistry and Chemical Engineering*, 41, 1844-1855, 2022.

[11]. Abdelfatah A. M., El-Maghrabi N., Mahmoud A. E. D., Fawzy M., "Synergetic effect of green synthesized reduced graphene oxide and nano-zero valent iron composite for the removal of doxycycline antibiotic from water," *Sci Rep,* 12, 19372, 2022.

[12]. Cao X., Wang H., Yang C., Cheng L., Fu K., Qiu F., "Nanoscale zero-valent iron supported on carbon nanotubes for polychlorinated biphenyls removal," *Desalination and Water Treatment,* 201, 173-186, 2020.

[13]. Nguyen P., Ha D., Nguyen T., La D., Cao H., Nguyen P., "Study on MIL-100 (Fe)/GNPs composite process to treat wastewater of dyes," *Vietnam Journal of Catalysis and Adsorption,* 9, 95-99, 2020.

[14]. Zhong L., Pham T. H. M., Ko Y., Züttel A., "Graphene nanoplatelets promoted CoO-based catalyst for low temperature CO_2 methanation reaction," *Front. Chem. Eng.,* 5, 1160254, 2023.

[15]. Rakočević L., Golubović J., Radović D. V., Rajić V., Štrbac S., "A comparative study of hydrogen evolution on Pt/GC and Pt/GNPs in acid solution," *International Journal of Hydrogen Energy*, 51, 1240-1254, 2024.

[16]. El-Shafei M., Hamdy A., Hefny M., "Zero-valent iron nanostructures: synthesis, characterization and application," *Journal of Environment and Biotechnology Research,* 7, 1, 1-10, 2018.

THÔNG TIN TÁC GIẢ

Nguyễn Mạnh Hà[1], Nguyễn Đức Kiên[1], Lê Hải Yến[1], Nguyễn Thu Trang[1], Vũ Minh Châu[2], Nguyễn Thị Hoài Phương[2]

[1]Khoa Công nghệ Hóa, Trường Đại học Công nghiệp Hà Nội

[2]Trung tâm Nhiệt đới Việt - Nga